A new strategy for evaluating the LO HVP contribution to $(g-2)_\mu$ on the lattice

K. Maltman[*]
York University and CSSM, University of Adelaide
E-mail: kmaltman@yorku.ca

M. Golterman
San Francisco State University
E-mail: maarten@stars.sfsu.edu

S. Peris
Universitat Autònoma de Barcelona
E-mail: peris@ifae.es

A highly physical model of the subtracted $I = 1$ vector polarization, obtained using a dispersive representation with precise hadronic τ decay data as input, is used to investigate systematic issues in the lattice evaluation of the leading order hadronic vacuum polarization contribution to the anomalous magnetic moment of the muon. The model is also employed to study possible resolutions of these problems. A hybrid approach to analyzing lattice data, involving low-order Padé, low-degree conformal-variable polynomial, or supplemented NNLO ChPT fits for Q^2 below $\sim 0.1 - 0.2$ GeV^2 and direct numerical integration of lattice data above this point, is shown to bring the systematic issues identified under control at the sub-1% level.

The 32nd International Symposium on Lattice Field Theory
23-28 June, 2014
Columbia University New York, NY

[*]Speaker.

1. Introduction

The muon anomalous magnetic moment, $a_\mu \equiv (g-2)_\mu/2$, is currently measured to 0.5 ppm [1], with plans for a further factor of 4 improvement in the upcoming Fermilab experiment. This improvement is of particular interest given the $3.3 - 3.6\,\sigma$ discrepancy between the current determination and the Standard Model (SM) prediction [2]. After the purely QED contribution [3], the next largest SM contribution is that from the leading order (LO) hadronic vacuum polarization (HVP), $a_\mu^{LO,HVP}$. The SM version of $a_\mu^{LO,HVP}$ is given by the weighted dispersive integral

$$\left(\frac{m_\mu^2}{12\pi^3} \right) \int_{m_\pi^2}^\infty ds \frac{K(s)}{s} \sigma_{had}^0(s) \,, \tag{1.1}$$

with $\sigma_{had}^0(s)$ the bare $e^+e^- \to hadrons$ cross-section and $K(s)$ a known kernel varying monotonically from 0.4 to 1 as s varies from m_π^2 to ∞. The error on $a_\mu^{LO,HVP}$ is the largest of the errors entering the SM prediction [2] and hence a key target for near-term improvement. Discrepancies between the results of different experiments for the key $e^+e^- \to \pi^+\pi^-$ cross-sections [4] also represent an important complication for the dispersive evaluation.

The deviation of the experimental result from the SM prediction, and the role played by the error on $a_\mu^{LO,HVP}$, have led to interest in an independent determination of $a_\mu^{LO,HVP}$ from the lattice [5, 6, 7, 8, 9, 10]. Such a determination is made possible by the alternate representation [5, 11]

$$a_\mu^{LO,HVP} = -4\alpha_{EM}^2 \int_0^\infty dQ^2 f\left(Q^2\right) \hat{\Pi}\left(Q^2\right) \,, \tag{1.2}$$

with the integral running over Euclidean Q^2, $\hat{\Pi}(Q^2) = \Pi(Q^2) - \Pi(0)$ the subtracted electromagnetic (EM) current polarization and $f\left(Q^2\right)$ a known kernel which makes the integrand very strongly peaked at low Q^2 ($Q^2 \simeq m_\mu^2/4$).

The lattice evaluation is complicated by the fact that, for current simulations, the discrete Q^2 available on the lattice provide rather coarse coverage of the critical low-Q^2 region, with the lowest accessible Q^2 lying above the peak of the integrand in Eq. (1.2) and the errors at the lowest few Q^2 points typically large (see, *e.g.*, Fig. 2). These limitations make an accurate determination of $a_\mu^{LO,HVP}$ by direct numerical integration of lattice data impossible at present. The problem is dealt with by fitting a continuous form to $\hat{\Pi}(Q^2)$ and using the resulting fitted version in place of $\hat{\Pi}(Q^2)$ in Eq. (1.2). Existing lattice analyses have typically employed fit ranges extending up to $Q^2 \sim 1$ or 2 GeV^2, the much smaller errors at larger Q^2 serving to sharpen the determinations of the parameters employed in the fits. The very good χ^2/dof's typically obtained, however, provide no information about the reliability of the extrapolation of the fits to the very low-Q^2 region most relevant to $a_\mu^{LO,HVP}$. The reason is as follows. With $\rho(s) \geq 0$ the EM current spectral function, $\hat{\Pi}(Q^2)$ satisfies the dispersion relation

$$\hat{\Pi}(Q^2) = -Q^2 \int_{th}^\infty ds \frac{\rho(s)}{s(s+Q^2)} \,, \tag{1.3}$$

with th the threshold. The magnitudes of derivatives of all orders of $\hat{\Pi}(Q^2)$ with respect to Q^2

$$|d^n\hat{\Pi}(Q^2)/(dQ^2)^n| = n! \int_{th}^\infty ds\, \rho(s)/(s+Q^2)^{n+1} \,, \tag{1.4}$$

are thus uniformly smaller at high Q^2 than low Q^2. Fits to $\hat{\Pi}(Q^2)$ over a wide range of Q^2 therefore suffer from a potential systematic bias in which the much more numerous low-error, high-Q^2 points, which typically dominate the fit, produce an underestimate of the curvature of $\hat{\Pi}(Q^2)$ at low Q^2 and hence an unreliable extrapolation into the very low-Q^2 region. This issue has been investigated in Refs. [8, 10], using a highly physical model of the flavor *ud* $I = 1$ vector (V) current analogue, $\hat{\Pi}^{I=1}(Q^2)$, of $\hat{\Pi}(Q^2)$. The results of this investigation are outlined in Sec. 2.

The spectral function, $\rho^{I=1}(s)$, of $\hat{\Pi}^{I=1}(Q^2)$, appearing in the $I = 1$ analogue of Eq. (1.3), is experimentally determinable for $s < m_\tau^2$ from the inclusive *ud* V hadronic τ decay distribution [12], and modelled for $s > m_\tau^2$ as a sum of 5-loop $D = 0$ OPE [13] and residual duality-violating (DV) contributions, the latter treated using a large-N_c and Regge motivated model with parameters obtained in the finite energy sum rule analyses of Ref. [14]. The region $s > m_\tau^2$ plays a very small role at the low Q^2 relevant to $a_\mu^{LO,HVP}$, making the resulting $\hat{\Pi}^{I=1}(Q^2)$ model a highly physical one for use in quantitative studies of the systematics of fit approaches employed in earlier lattice analyses.

In what follows, $\hat{a}_\mu^{LO,HVP}$ denotes the *ud* V analogue of $a_\mu^{LO,HVP}$, $\hat{a}_\mu^{LO,HVP}[Q_{min}^2, Q_{max}^2]$ the contribution from the interval $Q_{min}^2 \leq Q^2 \leq Q_{max}^2$ in the analogue of Eq. (1.2), and $\hat{a}_\mu^{LO,HVP}[Q_{max}^2] \equiv \hat{a}_\mu^{LO,HVP}[0, Q_{max}^2]$. We also employ a set of fake *ud* V "lattice data" obtained by drawing a random sample from a multivariate Gaussian distribution generated using central values from the dispersive model for $\hat{\Pi}^{I=1}(Q^2)$ and the Q^2 set and covariance matrix of a $64^3 \times 144$ MILC ensemble with periodic boundary conditions, lattice spacing $a \approx 0.06$ fm and $m_\pi \approx 220$ MeV [15].

2. The systematic problem and a hybrid strategy for its solution

In what follows, we investigate the systematic issues raised above using the dispersive $I = 1$ model and the fake lattice data generated from it. To make the impact on the accuracy with which $\hat{a}_\mu^{LO,HVP}$ can be evaluated as transparent as possible, we will quote all errors as fractions of the full LO HVP contribution, $\hat{a}_\mu^{LO,HVP}$. We assume that $\Pi(0)$, needed to construct $\hat{\Pi}(Q^2)$ from the computed lattice $\Pi(Q^2)$, can be determined with sufficient accuracy, referring the reader to Ref. [10] for further discussion.
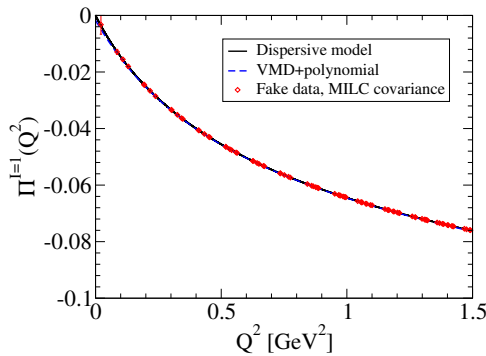

Figure 1: VMD+ fit (blue dashed curve), fake lattice data (red points) and underlying dispersive model (black solid curve) for $\hat{\Pi}^{I=1}(Q^2)$, $0 < Q^2 \leq 1$ GeV^2
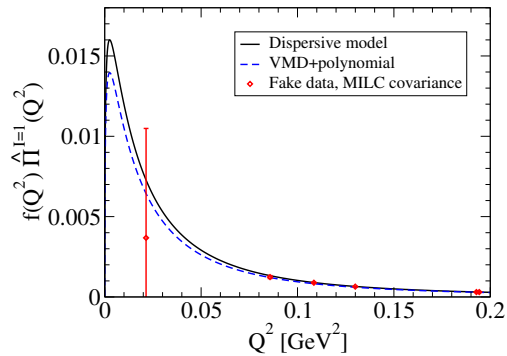
Figure 2: VMD+ fit (blue dashed curve), fake lattice data (red points) and underlying dispersive model (black solid curve) for $f(Q^2)\hat{\Pi}^{I=1}(Q^2)$, $0 < Q^2 \leq 0.2$ GeV^2

Fig. 1 shows the result of a fit to the fake lattice data on the interval $0 < Q^2 < 1$ GeV^2 using a form, "VMD+" (VMD plus a linear polynomial in Q^2), used previously in the literature. The quality of the fit is evidently very good. However, if we investigate how safe it is to extrapolate the fit into the region of the peak of the integrand in the $I = 1$ analogue of Eq. (1.2), we find the result shown in Fig. 2 [8]. The fit significantly underestimates the integrand in the region of the peak and produces an estimate for $\hat{a}_\mu^{LO,HVP} \sim 11\%$ lower than the exact underlying model value [8]. Even worse, the "pull" for this fit (the deviation of the fit estimate from the underlying model value, in units of the propagated fit error) is 18, making it clear that the in-principle systematic problem identified in Sec. 1 is, in general, numerically very significant. The level of the problem depends on the fit form employed. For example, employing instead the $[1,2]$ version of the Padés advocated in Ref. [7] on the same interval, one obtains a pull of 0.5 [8]. The potential systematic bias is, however, still present: if one fits the same $[1,2]$ Padé on the slightly enlarged interval $0 < Q^2 < 1.5$ GeV^2, and hence includes additional low-error, high-Q^2 points, the pull increases to 4 [8]. While the dispersive model can, of course, be used to quantify the systematic error associated with the use of any fit form choice, developing a strategy that focusses the use of fitting as much as possible on the low-Q^2 region which dominates $a_\mu^{LO,HVP}$ obviously represents a more attractive option.
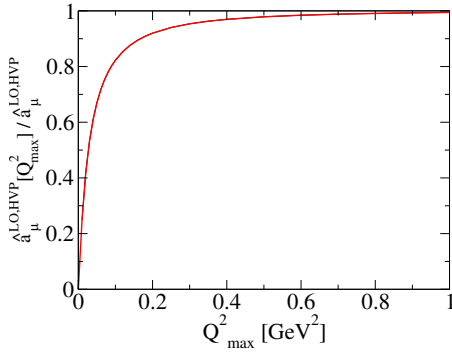

Figure 3: The accumulation of $\hat{a}_\mu^{\text{LO,HVP}}$ as a function of Q_{max}^2
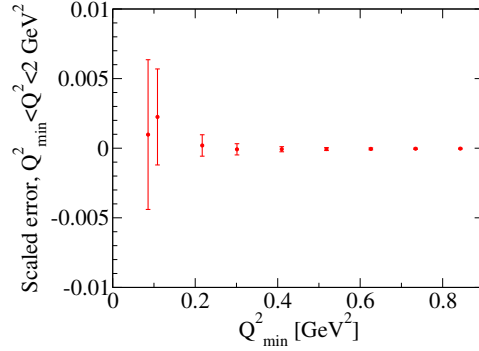

Figure 4: Systematic and statistical errors on the trapezoid-rule evaluation of $\hat{a}_\mu^{\text{LO,HVP}}[Q_{min}^2, 2\,\text{GeV}^2]$

Fig. 3 shows the accumulation of the fractional partial contribution, $\hat{a}_\mu^{LO,HVP}[Q_{max}^2]/\hat{a}_\mu^{LO,HVP}$, as a function of Q_{max}^2. We see that over 80% (90%) of the total is accumulated below $Q_{max}^2 = 0.1$ (0.2) GeV^2. The low-Q^2 domination of the Euclidean integral is thus much stronger than the low-s domination of the dispersive integral, Eq. (1.1), where one would have to integrate to ~ 1 (~ 1.5) GeV^2 to reach 80% (90%) of the total. This is a useful feature of the lattice formulation since one expects $\hat{\Pi}(Q^2)$ to be very accurately representable with few-parameter forms in such a small Q^2 interval. It also shows that considerably lower accuracy can be tolerated for the small contributions from Q^2 above $0.1 - 0.2$ GeV^2 than for the much larger low-Q^2 ones. It thus becomes relevant to investigate the accuracy with which higher-Q^2 contributions can be evaluated via direct numerical integration of existing lattice data. The results of this investigation, performed using the fake lattice data, are presented in Fig. 4, the central values showing the systematic error, resulting from the use of the trapezoid-rule approximation for $\hat{a}_\mu^{LO,HVP}[Q_{min}^2, 2\,\text{GeV}^2]$, and the error bars the corresponding propagated statistical errors (the covariance matrix of the fake data is, by construction, the MILC

covariance matrix used to generate the data). Direct numerical integration is found to provide a determination of the $Q^2 > Q^2_{min}$ contribution accurate to well below 1% of $\hat{a}^{LO,HVP}_\mu$ for Q^2_{min} down to ~ 0.1 GeV^2 [10].

In light of this observation, we focus on strategies for reliably representing the subtracted polarization in the region below $Q^2 \sim 0.1 - 0.2$ GeV^2. We have identified three approaches capable of producing determinations of $\hat{a}^{LO,HVP}_\mu[Q^2_{max}]$ with an accuracy below 1% of $\hat{a}^{LO,HVP}_\mu$ [10]. The first uses low-order Padés, the second low-degree polynomials in the conformal variable

$$w(Q^2) = \left[1 - \sqrt{1 + z(Q^2)}\right] \Big/ \left[1 + \sqrt{1 + z(Q^2)}\right], \quad z(Q^2) = \frac{Q^2}{4m_\pi^2}, \tag{2.1}$$

and the third a supplemented form of NNLO ChPT. We discuss each of these briefly in turn.

In the case of the Padés, we first consider the "one-point Padé" representations, constructed from the derivatives of $\hat{\Pi}^{I=1}(Q^2)$ with respect to Q^2 at $Q^2 = 0$. The required derivatives are easily determined from the dispersive representation in the model case, and have been argued to be determinable on the lattice from even-order Euclidean time moments of the zero-spatial-momentum current-current two-point functions [9]. In what follows, $[M,N]_H$ denotes the representation of $\hat{\Pi}^{I=1}(Q^2)$ as a quotient of polynomials of degree M and N. Fig. 5 shows the comparison of the $[1,0]_H$, $[1,1]_H$, $[2,1]_H$ and $[2,2]_H$ one-point Padés to the underlying dispersive model for $0 < Q^2 < 0.4$ GeV^2. Evidently even the $[1,1]_H$ form provides an excellent representation below $Q^2 \sim 0.2$ GeV^2. The corresponding errors on $\hat{a}^{LO,HVP}_\mu[Q^2_{max}]/\hat{a}^{LO,HVP}_\mu$ are shown in Fig. 6. The $[1,1]_H$ form yields a result accurate to $\sim 0.3\%$ ($\sim 0.5\%$) for $Q^2_{max} = 0.1$ (0.2) GeV^2. These numbers are reduced to $\sim 0.06\%$ and $\sim 0.2\%$ for the $[2,1]_H$ Padé. If one wished, as in Ref. [9], to use a one-point Padé to evaluate $\hat{a}^{LO,HVP}_\mu[Q^2_{max}]$ out to much larger Q^2_{max}, e.g., ~ 2 GeV^2, we find the $[2,2]_H$ form would be required to bring the systematic error down to the sub-percent level [10].
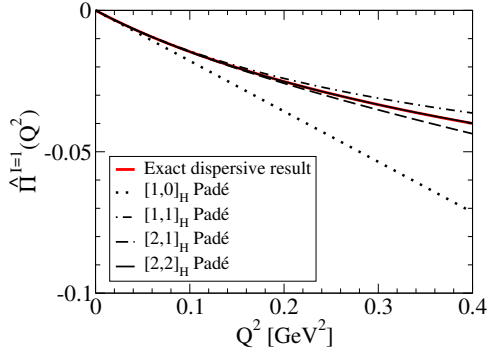

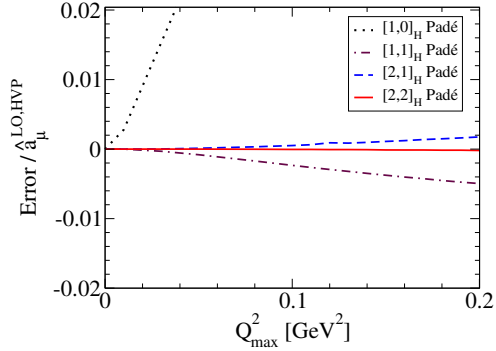**Figure 5:** Low-Q^2 comparison of one-point Padé representations and the dispersive model for $\hat{\Pi}^{I=1}(Q^2)$

Figure 6: Deviations of one-point Padé estimates for $\hat{a}^{LO,HVP}_\mu[Q^2_{max}]/\hat{a}^{LO,HVP}_\mu$ on the interval $0 \le Q^2_{max} \le 0.2$ GeV^2

It is also possible to consider "multi-point Padés", Padés with coefficients obtained by fitting $\hat{\Pi}^{I=1}(Q^2)$ in an interval of Q^2. Since the low-Q^2 coverage is too sparse and the lowest-Q^2 errors too large to produce stable low-Q^2 fits of this type for the fake lattice data, we have investigated this possiblility using the dispersive *ud* V model itself, together with the covariances generated by the underlying dispersive representation. The results of fits to the model data at

$Q^2 = 0.10, 0.11, \cdots, 0.20$ GeV^2 show that, to achieve the same accuracy as achieved with a given one-point-Padé fit, it is necessary to go to a multi-point Padé one order higher. A multi-point $[2,1]_H$ Padé, which yields an accuracy of better than 0.45% on $\hat{a}_\mu^{LO,HVP}\left[Q_{max}^2\right]/\hat{a}_\mu^{LO,HVP}$ for $Q_{max}^2 \leq 0.2$ GeV^2, is required to reach sub-percent accuracy in this region for a fit of this type.
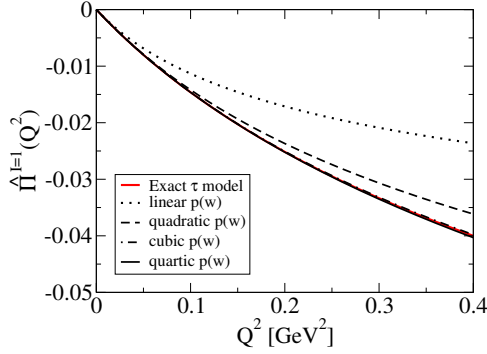

Figure 7: Comparison of conformal polynomial representations to the underlying dispersive model for $\hat{\Pi}^{I=1}(Q^2)$
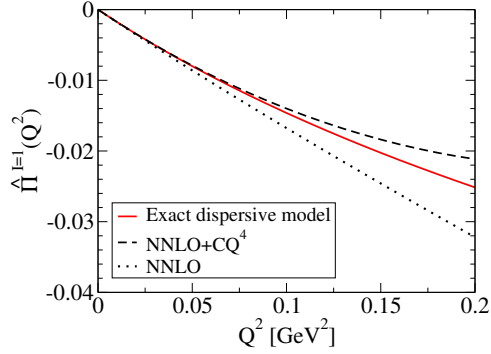
Figure 8: Comparison of the NN′LO and NNLO ChPT representations to the underlying dispersive model for $\hat{\Pi}^{I=1}(Q^2)$

The use of polynomials in the conformal variable w is motivated by the fact that the transformation $Q^2 \to w$ maps the entire cut Q^2-plane into the interior of the unit circle in the w-plane, with the cut mapped to the boundary. The Euclidean Q^2 entering the integral in Eq. (1.2) thus lie in the region of convergence of the Taylor series in w. The coefficients of polynomial-in-w representations of $\hat{\Pi}^{I=1}(Q^2)$ can, as in the Padé case, be obtained either in "one-point" form from the derivatives of $\hat{\Pi}^{I=1}(Q^2)$ with respect to Q^2 at $Q^2 = 0$, or in "multi-point" form from fits to $\hat{\Pi}^{I=1}(Q^2)$ on an interval of (low) Q^2. One-point-form results for polynomials linear, quadratic, cubic and quartic in w are compared to the underlying dispersive model in Fig. 7. Very accurate representations are seen to be achievable for Q^2 well beyond 0.2 GeV^2. For the quadratic case, the resulting accuracies on $\hat{a}_\mu^{LO,HVP}\left[Q_{max}^2\right]/\hat{a}_\mu^{LO,HVP}$ are 0.6% and 1% for $Q_{max}^2 = 0.1$ and 0.2 GeV^2, respectively. These numbers improve to 0.02% and 0.04% if the cubic representation (having the same number of parameters as a $[2,1]_H$ Pade) is used. As in the Padé case, we find that multi-point forms one order higher must be used to reach the same accuracy as achieved using a given one-point form for $Q_{max}^2 \leq 0.2$ GeV^2 [10].

The last of the low-Q^2 options we have considered is that provided by ChPT. The low-energy representation of $\hat{\Pi}^{I=1}(Q^2)$ is known to NNLO [16], and the model version of $\frac{d\hat{\Pi}^{I=1}}{dQ^2}(0)$ corresponds to a value of the relevant NNLO LEC, C_{93}^r, in good agreement with expectations based on dominance by the large ρ peak in $\rho^{I=1}(s)$. In the narrow width approximation, expanding the ρ propagator to one higher order yields an NNNLO contribution proportional to Q^4 which is numerically relevant already at $Q^2 \sim 0.1$ GeV^2. We have thus constructed a supplemented "NN′LO" form by adding a term CQ^4 to the known NNLO form. Fixing C_{93}^r and C to reproduce the first two derivatives of $\hat{\Pi}^{I=1}(Q^2)$ with respect to Q^2 at $Q^2 = 0$ yields the representation given by the dashed line in Fig. 8. The dotted line is the analogous pure NNLO result. The NNLO form produces 4% and 18% errors on $\hat{a}_\mu^{LO,HVP}[Q_{max}^2]/a_\mu^{LO,HVP}$ for $Q_{max}^2 = 0.1$ and 0.2 GeV^2, respectively, and is hence inadequate for our purposes. The corresponding errors for the NN′LO form are 0.6% and

1.4%, with only the former showing sub-percent accuracy. Since the accuracy of even the NN′LO representation begins to break down above $Q^2 \sim 0.1$ GeV^2, fixing the required LECs via fits to $\hat{\Pi}^{I=1}(Q^2)$ on an interval like $0.1 \leq Q^2 \leq 0.2$ GeV^2 is not an option in this case. We thus expect the ChPT representation to be less useful than the Padé and conformal-variable-polynomial representations, though it will provide cross-checks on the other methods. One place where the ChPT representation is, nonetheless, useful, is in providing an understanding of the dependence of the low-Q^2 contributions to $\hat{a}_\mu^{LO,HVP}$ on m_π^2 and m_K^2. We find that, for many of the simulations in the literature, m_π^2 is too large to allow a linear extrapolation to physical m_π^2.

References

[1] G.W. Bennett *et al.*, Phys. Rev. Lett. **92**, 161802 (2004); Phys. Rev. **D73**, 072003 (2006).

[2] See, e.g., F. Jegerlehner and A. Nyffeler, Phys. Rept. **477**, 1 (2009); M. Davier, *et al.*, Eur. Phys. J. C **71**, 1515 (2011) [Erratum-ibid. C **72**, 1874 (2012)]; T. Blum, *et al.*, arXiv:1311.2198 [hep-ph], and references therein.

[3] T. Aoyama, M. Hayakawa, T. Kinoshita and M. Nio, Phys. Rev. Lett. **109**, 111808 (2012).

[4] R. R. Akhmetshin *et al.* [CMD-2 Collaboration], Phys. Lett. **B648**, 28 (2007); M. N. Achasov, *et al.* [SND Collaboration], J. Exp. Theor. Phys. **103**, 380 (2006) [Zh. Eksp. Teor. Fiz. **130**, 437 (2006)]; D. Babusci, *et al.* [KLOE Collaboration], Phys. Lett. **B720**, 336 (2013); J. P. Lees, *et al.* [BaBar Collaboration], Phys. Rev. **D86**, 032013 (2012). See, in particular, Figs. 48 and 50 of the latter.

[5] T. Blum, Phys. Rev. Lett. **91**, 052001 (2003).

[6] C. Aubin and T. Blum, Phys. Rev. **D75**, 114502 (2007); X. Feng *et al.*, Phys. Rev. Lett. **107**, 081802 (2011); X. Feng *et al.*, PoS LATTICE **2012**, 174 (2012); P. Boyle, it et al., Phys. Rev. **D85**, 074504 (2012); T. Blum, *et al.*, PoS LATTICE **2012**, 022 (2012); M. Della Morte, *et al.*, JHEP **1203**, 055 (2012) and PoS LATTICE **2012**, 175 (2012); G. M. de Divitiis, *et al.*, Phys. Lett. B **718**, 589 (2012); X. Feng, *et al.*, Phys. Rev. **D88**, 034505 (2013); A. Francis, *et al.*, Phys. Rev. **D88**, 054502 (2013); C. Aubin, *et al.*, Phys. Rev. **D88**, 074505 (2013); F. Burger, *et al.*, JHEP **1402**, 099 (2014); H. Horch, *et al.*, PoS LATTICE **2013**, 304 (2013); E. de Rafael, Phys. Lett. **B736**, 522 (2014).

[7] C. Aubin, T. Blum, M. Golterman and S. Peris, Phys. Rev. D **86**, 054509 (2012).

[8] M. Golterman, K. Maltman and S. Peris, Phys. Rev. **D88**, 114508 (2013).

[9] B. Chakraborty, *et al.*, arXiv:1403.1778 [hep-lat];

[10] M. Golterman, K. Maltman and S. Peris, Phys. Rev. **D90**, 074508 (2014).

[11] B. E. Lautrup, A. Peterman and E. de Rafael, Phys. Rep. **3**, 193 (1972).

[12] Y.-S. Tsai, Phys. Rev. **D4**, 2821 (1971).

[13] P. A. Baikov, K. G. Chetyrkin and J. H. Kühn, Phys. Rev. Lett. **101**, 012002 (2008).

[14] D. Boito, *et al.*, Phys. Rev. **D85**, 093015 (2012).

[15] MILC collaboration, http://physics.indiana.edu/∼sg/milc.html .

[16] G. Amoros, J. Bijnens and P. Talavera, Nucl. Phys. **B568** 319 (2000).